Brownness of Organics in Anthropogenic Biomass Burning Aerosols over South Asia

Chimurkar Navinya[1], Taveen Singh Kapoor[2], Gupta Anurag[1,3], Chandra Venkataraman[1,4,*], Harish C. Phuleria[1,3], Rajan K. Chakrabarty[2,*]

[1] Interdisciplinary Program in Climate Studies, Indian Institute of Technology Bombay, Mumbai, India – 400076.
[2] Center for Aerosol Science and Engineering, Department of Energy, Environmental and Chemical Engineering, Washington University in St. Louis, St. Louis, MO, USA – 63130.
[3] Environmental Science and Engineering Department, Indian Institute of Technology Bombay, Mumbai, India – 400076.
[4] Department of Chemical Engineering, Indian Institute of Technology Bombay, Mumbai, India – 400076.

Correspondence to: Rajan K. Chakrabarty (chakrabarty@wustl.edu) & Chandra Venkataraman (chandra@iitb.ac.in)

Abstract

In South Asia, biomass is burned for energy and waste disposal, producing brown carbon (BrC) aerosols whose climatic impacts are highly uncertain. To assess these impacts, a real-world understanding of BrC's physio-optical properties is essential. For this region, the order-of-magnitude variability in BrC's spectral refractive index as a function of particle volatility distribution is poorly understood. This leads to oversimplified model parameterization and subsequent underestimation of regional radiative forcing. Here we used the field-collected aerosol samples from major anthropogenic biomass activities to examine the methanol-soluble BrC optical properties. We show a strong relation between the absorption strength, wavelength dependence, and thermo-optical fractions of carbonaceous aerosols. Our observations show strongly absorbing BrC near the Himalayan foothills that may accelerate glacier melt, further highlighting the limitations of climate models where variable BrC properties are not considered. These findings provide crucial inputs for refining climate models and developing effective regional strategies to mitigate BrC.

Keywords: Brown carbon, Biomass fuels, Imaginary refractive index, Organic carbon

1. Introduction

Carbonaceous aerosols, such as black and organic carbon, make up most fine particulate matter ($PM_{2.5}$) emissions globally (Mcduffie et al., 2020; Roy et al., 2023; Kurokawa and Ohara, 2020; Crippa et al., 2018) and ~40% over South Asia (Tibrewal et al., 2024; Pandey et al., 2014; Sadavarte et al., 2019). Anthropogenic biomass usage for residential cooking and heating (Pandey et al., 2014; Habib et al., 2023; Navinya et al., 2023), residue burning for agricultural waste disposal (Kapoor et al., 2023b; Azhar et al., 2019) and biomass-fired brick kilns (Weyant et al., 2014; Tibrewal et al., 2023) are the common sources of these carbonaceous aerosols across South Asia (Tibrewal et al., 2024; Pandey et al., 2014; Sadavarte et al., 2019; Ohara et al., 2007) and many other developing countries (Bonjour et al., 2013; Yevich and Logan, 2003; Mcduffie et al., 2020). These aerosols perturb the Earth's energy balance, depending on their mixing state, size distribution, wavelength dependence of optical properties, and absorption

strength (Zhang et al., 2020; Neyestani and Saleh, 2022; Brown et al., 2018; Arola et al., 2015; Bond and Bergstrom, 2006). However, the extent of this perturbation remains uncertain (Szopa et al., 2021; Gliß et al., 2021). Over the last two decades, extensive research has focused on the climate impact of highly absorbing black carbon (BC) (Bond et al., 2013). In contrast, the
45   climate implications of light-absorbing organic carbon (OC), termed brown carbon (BrC), have received relatively less attention and are thus less certain (Saleh et al., 2018; Brown et al., 2018; Saleh, 2020). The chemical composition of BrC varies significantly, and consequently its optical properties, as reported across previous studies, span orders of magnitude in the imaginary refractive index (k) values that determine its light absorbing strength (Chakrabarty
50   et al., 2023; Choudhary et al., 2021, 2018, 2017; Dey et al., 2021; Kapoor et al., 2023a; Kirillova et al., 2016; Rana et al., 2020; Rathod et al., 2017; Saleh et al., 2018, 2014; Srinivas and Sarin, 2014). Previous studies often measured aged ambient BrC that are weakly absorbing ($k_{BrC,550}$ <0.01) due to photobleaching (Sumlin et al., 2017), hence some climate impact assessment studies have considered BrC as a weakly or non-absorbing particle (Lee et al., 2010;
55   Sand et al., 2021; Zhang et al., 2020). However, this underestimates the impact of freshly emitted BrC that has high absorption strength ($k_{BrC,550}$ > 0.1) and resists photobleaching, resulting in extended atmospheric lifetime (Chakrabarty et al., 2023). Furthermore, the formation of light-absorbing secondary BrC and the enhancement of BC absorption due to OC coating (Rastogi et al., 2021; Bhowmik et al., 2024; Kapoor et al., 2022) add complexity to
60   radiative transfer models.

BrC has a wide range of absorption strength; studies show $k_{BrC,550}$ varying from ~0.007 (Islam et al., 2022) to ~0.2 (Chakrabarty et al., 2023). In addition to the different methods used to derive BrC optical information, such variation is associated with the different combustion conditions (Saleh et al., 2018), ageing of BrC (Sumlin et al., 2017; Dasari et al., 2019;
65   Romonosky et al., 2016; Chen et al., 2021), and secondary reactions (Wang et al., 2020; Kroll et al., 2007; Kroll and Seinfeld, 2008; Hecobian et al., 2010). An experimental study explained that the progressive transformation of BC precursors to BC results from different combustion conditions, which create the BrC-BC light-absorption continuum (Saleh et al., 2018). This continuum shows an increase in the absorption strength of carbonaceous aerosols that is
70   associated with a decrease in wavelength dependence (w), solubility, and volatility (Saleh, 2020). Recent studies also observed such a relationship, but for a smaller range of k_{BrC} (<0.01) (Devaprasad et al., 2024; Luo et al., 2022). However, information about real-world source specific BrC absorption and its position in the BrC-BC continuum is lacking. Understanding this light absorption continuum alongside carbonaceous aerosol emissions aids BrC
75   parameterization in climate models (Zhang et al., 2020; Saleh et al., 2014). Presently, because source specific BrC information is absent from emission inventories, many climate models inadequately account for BrC. Studies have used the BrC to BC ratio along with the k_{BrC} to understand its direct radiative effect (Park et al., 2010; Feng et al., 2013). Furthermore, other studies (Zhang et al., 2020; Neyestani and Saleh, 2022; Brown et al., 2018) have employed
80   BrC parameterization schemes based on laboratory-generated data to address the climate impact of BrC, but this approach might not adequately represent real-world biomass burning conditions (Saleh et al., 2014; Lu et al., 2015). Hence, regions with high OC emissions and stronger BrC (S-BrC), also known as dark BrC ($k_{BrC,550}$ > 0.1), could have a high climate impact

due to persistent BrC, possibly underestimated in the absence of regional source specific BrC data.

The recent Carbonaceous Aerosol Emissions, Source Apportionment and Climate Impacts (COALESCE) field emission measurement campaigns and questionnaire surveys in India (Navinya et al., 2023; Kapoor et al., 2023b; Tibrewal et al., 2023; Habib et al., 2023) have prepared a comprehensive inventory encompassing both formal (transportation, industries and power generation) and informal (residential, agricultural residue burning, and brick production) emission sectors (Venkataraman et al., 2020; Tibrewal et al., 2024). It recognizes the substantial contribution of anthropogenic $PM_{2.5}$ in India arising from biomass fuel burning practices for residential cooking and agricultural residue burning (Kapoor et al., 2023b; Tibrewal et al., 2024; Habib et al., 2023). Recent studies have highlighted considerable biomass consumption for residential heating and brick production (Tibrewal et al., 2023; Navinya et al., 2023). Figure 1 shows 91% of the OC emissions (3 Tg y^{-1}) over India are from three sources: residential cooking (COOK), heating (HEAT), and agricultural residue burning (AGRI), with most emissions from the Indo-Gangetic plain (~50%) (Tibrewal et al., 2024). The unexplored climate impacts of OC emitted from these biomass-based sources make the Indian subcontinent particularly prone to environmental challenges.
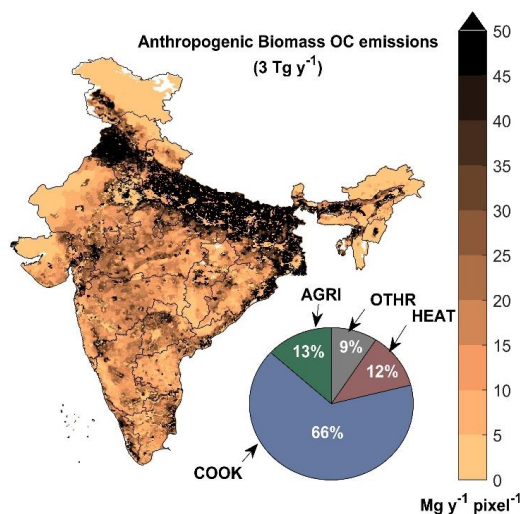
Figure 1. The spatial distribution of OC emissions (Mg y^{-1} pixel^{-1}) from three major sources—agricultural residue burning (AGRI), residential cooking (COOK) and residential heating (HEAT)—covers ~91% of the total OC emissions (3.3 Tg y^{-1}) over India. OC emissions are taken from the Carbonaceous Aerosol Emissions, Source Apportionment and Climate Impacts (COALESCE) Speciated Multipollutant Generator (SMoG)-India emission inventory for the year 2019 (Tibrewal et al., 2024). Here, the pixel size is 5×5 km. The pie chart represents the shares of anthropogenic biomass burning sources in the total OC emissions over India. Other sources (OTHR) of OC include brick production, transportation, industries, and power generation.

This study leverages samples of aerosol particle emissions collected on filter substrates during the COALESCE field campaign to propose a hypothesis regarding the BrC-BC continuum in BrC optical properties. Using a UV-Vis spectrophotometer, it examines BrC derived from major biomass fuel sources such as cooking, heating, agricultural residue burning, and brick production. The study aims to connect BrC with the thermo-optically resolved carbon fractions to parameterize BrC absorption over South Asia. Further, it endeavours to couple source specific BrC properties with the BC-to-organic-aerosols (OA) ratio to explore the spatial variability of the absorption properties of BrC emitted across India.

2. Data and Methods

2.1. Data Collection

The field-based emissions measurement campaign (Figure S2) was conducted from Oct-2021 to Apr-2022 in rural parts of Gujarat and Maharashtra, two western India states. These locations were selected based on their representativeness for the fuels and devices commonly used in South Asia based on previous studies (Navinya et al., 2023; Kapoor et al., 2023b; Tibrewal et al., 2023; Habib et al., 2023). The primary aim of this campaign was to capture physical, chemical, and optical information about the emissions from biomass sources: agricultural residue burning, brick production from clamps, cooking, and heating. The emission measurement sampler used in this campaign was equipped with real-time instruments, along with a gravimetric module that collected particulate emissions on quartz filter paper for offline lab-based analyses. The multi-arm inlet probe was placed 1-1.5m above source (Figure S2), adapted from Roden et al., 2006. The sampler is fully described in previous studies (Venkataraman et al., 2020; Kumari et al., 2021). For this study, we have only utilized quartz filters from 14 different fuel and source combinations (Table S1) to understand soluble BrC absorption and total OC concentration.

2.2. Estimation of BrC Properties

We used 4.5 ml of methanol solvent and dissolved two 0.25-inch diameter punches of quartz filters. After 1 hour of sonication, the extracted solvent was passed through a 0.22 μm polytetrafluoroethylene membrane syringe filter (Fisherbrand™) to remove insoluble debris. The absorption of this methanol-soluble OC (considered as BrC absorption) was estimated by using a UV-visible spectrophotometer (LAMBDA 35, PerkinElmer) with a working range of 300 nm to 900 nm and a spectral resolution of 1 nm. The equation shown below was used to estimate the absorption at any given wavelength (Chakrabarty et al., 2023; Sarkar et al., 2019; Satish and Rastogi, 2019; Srinivas and Sarin, 2013, 2014; Bikkina et al., 2020; Boreddy et al., 2021; Choudhary et al., 2017, 2018, 2021, 2022; Dasari et al., 2019; Dey et al., 2021; Kirillova et al., 2016; Mukherjee et al., 2020; Rajeev et al., 2022; Rastogi et al., 2021; Rathod et al., 2017; Rana et al., 2020; Shamjad et al., 2016b, 2018).

$$b_{abs,BrC,\lambda} = \frac{(A_\lambda - A_{700}) \times V_{Extract} \times \ln(10)}{V_{Sampled} \times L \times f_{filter\ area}}$$

(1)

150   In equation 1, A_λ is absorbance at wavelength λ, $V_{Extract}$ is the volume of solvent extract used
        (4.5 ml in this study), $V_{Sampled}$ is the volume of air sampled, $f_{filter\ area}$ is the fraction of filter
        area used for the analysis, and L is the optical path length (0.01 m). Given that soluble BrC
        does not absorb at 700 nm and longer wavelengths or, at best, absorbs very little, the absorption
        at 700 nm (A_{700}) was used to normalize absorbance to account for signal drift within the
155   instrument, which is a limitation of this method. In this study, the estimated BrC only includes
        the methanol-soluble component and may not fully represent total BrC, including its insoluble
        components. The estimated BrC absorption could be underestimated due to excluded insoluble
        BrC and tarball structures, which possess high absorption strength (Corbin et al., 2019;
        Chakrabarty et al., 2023, 2010). The underestimation may be more pronounced within the dark-
160   BrC region but comparatively lower in other BrC categories (figure 2), considering the inverse
        relationship between BrC absorption strength and solubility. (Saleh, 2020). In this study only
        two data points, observed marginally in the dark-BrC region, might be affected.

        Quartz filters were examined using a Magee Scientific DRI multi-wavelength thermo-optical
        carbon analyser with the IMPROVE-A protocol to estimate the elemental (EC) and organic
165   carbon (OC) concentrations (Chow et al., 2007). Thermo-optically resolved carbon fractions
        (OC1, OC2, OC3, OC4, EC1, EC2, and EC3) were used after pyrolytic correction to
        reconstruct the total organic carbon and total elemental carbon fractions (Chow et al., 2007).
        These fractions are associated with the volatility of the OC (Kapoor et al., 2023a; Shetty et al.,
        2023; Tohidi et al., 2022; Vodička et al., 2015; Soleimanian et al., 2019; Ma et al., 2016), as
170   these OC fractions are measured under increasing temperature peaks (140, 280, 480, & 580°C)
        during thermo-optical analysis. Hence, OC1 exhibits relatively higher volatility compared to
        OC2, while OC2 is more volatile than OC3, and so forth. In this study, pyrolysis corrected EC
        was treated as a proxy of BC to facilitate the comparison with other studies. The uncertainty
        associated with OC and EC measurements are 5 and 10% respectively (Cheng et al., 2021; DRI
175   Manual, 2015). Assuming a 10% uncertainty in absorption coefficient and a manufacturer-
        assigned uncertainty of 5% in OC concentration, the overall uncertainty remains below 10%
        for the k, consistent with previous study (Cheng et al., 2021).

        Furthermore, OC concentration and $b_{abs,BrC,\lambda}$ were used to calculate the mass absorption
        coefficient (MAC$_{BrC,\lambda}$). The imaginary refractive index of BrC (k$_{BrC,\lambda}$) was estimated by
180   considering the density (ρ) of freshly emitted OC to be 1.5 kg m^{-3} (Liu et al., 2013; Shamjad
        et al., 2016), using the following relation (Jennings et al., 1979):

$$k_\lambda = \frac{\rho \times \lambda \times MAC_\lambda}{4\pi}$$

(2)

        The same equation was used in many previous studies, some of which cover the same
185   geographic region (Shamjad et al., 2018; Bikkina and Sarin, 2019; Shamjad et al., 2016b; Rana
        et al., 2020; Liu et al., 2013; Zhang et al., 2020). In addition, an absorption Angstrom exponent
        (AAE) between 365 and 550 nm (AAE$_{365/550}$ = -ln[b$_{abs,BrC,365}$/b$_{abs,BrC,550}$]/ln[365/550]) was also
        estimated to understand the spectral dependence of the BrC absorption coefficient. Similarly,
        w (AAE-1) indicates the spectral dependence of the imaginary refractive index (w) between

190 365 nm (a commonly used wavelength for studying BrC absorption) and 550 nm (the peak of solar radiation intensity). In this study, we have used w and k for the ease of comparison with previous study (Saleh et al., 2014; Lu et al., 2015; Luo et al., 2022; Saleh et al., 2018), however, AAE and MAC can also be used interchangeably.

195 **2.3. Spatial variation of BrC absorption**

The relationship between fuel and source averaged $k_{BrC,550}$ and the BC to OA ratio ($k_{BrC,550}$ = 0.0365($\pm$0.006)$\times$(BC/OA) + 0.0047($\pm$0.0037), R^2 = 0.93) was established using field-collected fuel samples. Similarly, w was also calculated as a function of the BC to OA ratio (w=5.355($\pm$0.50)$\times$exp(-0.428($\pm$0.25)$\times$(BC/OA), R^2=0.60). Here, OA was derived by

200 multiplying OC by a factor of 1.8, a methodology consistent with previous studies (Turpin et al., 2001; Chow et al., 2015; Navinya et al., 2020; Provençal et al., 2017; Kumar et al., 2023). Although this factor does not impact the R-square (R^2) of the relationship, it facilitates comparisons with other studies that have utilized the BC to OA ratio to derive $k_{BrC,550}$. The spatial distribution of BC and OC emissions from the SMoG-India emission inventory

205 (Tibrewal et al., 2024) was integrated into the equation, after converting OC into OA using the same factor, to calculate the nationwide $k_{BrC,550}$ and w for the major (~90%) OC emitting sources: AGRI, COOK, and HEAT. Additionally, we derived overall k_{BrC} and w values through a weighted averaging approach, incorporating OC emissions (Figure S5) as weights, along with source-specific information (Figure S3). BRICK (brick production) was omitted because field-

210 based samples were limited to clamp kilns, but not available for other major brick production technologies, including Bull's trench kilns and vertical shaft brick kilns (Weyant et al., 2014; Tibrewal et al., 2024, 2023).

3. Results and Discussion

215 **3.1. BrC-BC Absorption Continuum**

The measured $k_{BrC,550}$ values varied from 0.0007 to 0.1199, while w ranged from 7.52 to 1.00, highlighting inverse dependence of k_{BrC} on w (Figure 2). A previous study using synthetic fuels under different combustion conditions reported a similar observation, based on experimental measurements (Saleh et al., 2018). In this study, different field-collected sources and fuels

220 reflected real-world variations in burning practices. An equation fitted to the data (w = 0.1917/($k_{BrC,550}$ + 0.02886)) has a correlation coefficient of 0.76, and an extension of this curve with 95% prediction bounds overlaps the BC absorption region (k_{550} = 0.6-0.8 and w = ~0-0.2) (Bond and Bergstrom, 2006; Saleh et al., 2018; Liu et al., 2018; Gyawali et al., 2013). Figure 2 depicts data primarily falling within three major classes of BrC (weak, moderate and strong);

225 nevertheless, some data points do not fall within any of the three classes defined by Saleh (2020).

The thermo-optically resolved carbon fractions show a decline in the total OC fraction, mainly OC3 and OC4 (a relatively low volatile fractions) with increasing BrC absorption strength (Figure 3a). A simultaneous increase of EC highlights the dominance of BC absorption as the

230 strength of BrC absorption increases, as also reported previously (Saleh et al., 2014; Chakrabarty et al., 2023). Such relationships between BC, OC and BrC properties are useful in parameterizing the BrC absorption in climate models.
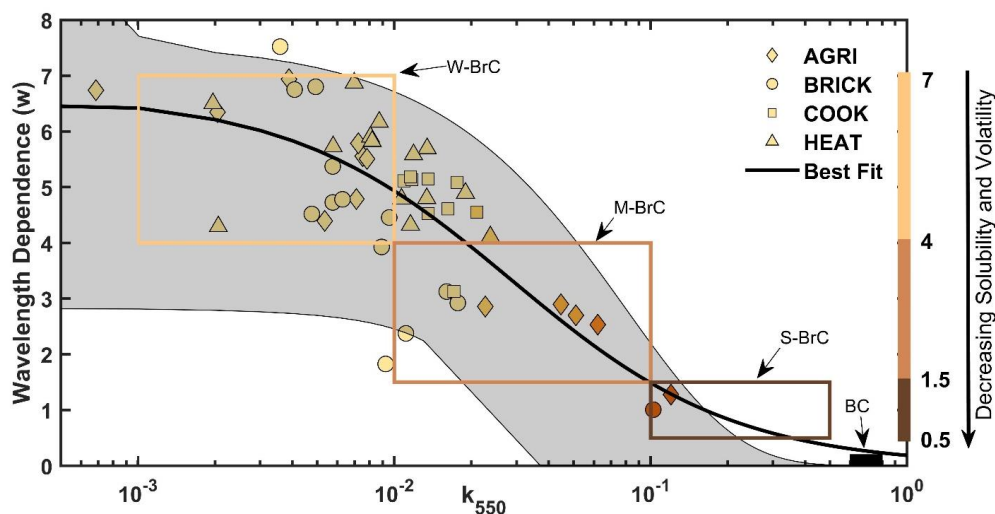
Figure 2. BrC-BC light absorption continuum in semi-log scale, showing the wavelength
235 dependence (w = AAE-1) of the imaginary part of the refractive index (k_{550}) versus the imaginary part of the refractive index at 550 nm (k_{550}), $w = 0.1917(\pm 0.074)/(k_{BrC,550} + 0.02886(\pm 0.014))$. Here, the BC region lies between k_{550} = 0.6 - 0.8 and w = 0 - 0.2. The BrC classes are defined per Saleh, (2020): strongly absorbing BrC (S-BrC), moderately absorbing BrC (M-BrC), and weakly absorbing BrC (W-BrC). Arrow in the right indicates reduction in
240 the solubility and volatility with increase in k_{550} (Saleh, 2020). The shaded grey area represents the continuum reported by previous studies (Saleh et al., 2014; Lu et al., 2015; Luo et al., 2022; Saleh et al., 2018), and the equations for the shaded area are given in the supplementary information, S1 and figure S1. The right axis displays the range of wavelength dependence for the three BrC classes.

245

3.2. Source Specific BrC

We observed that the variability of source specific BrC properties is larger within a source category than among different source categories. Figure 3b shows no significant changes in $k_{BrC,550}$ among different source categories, however, there are much larger differences among
250 individual data points in a source category, because of varying fuels, meteorology, and burning practices. The $k_{BrC,550}$ means from agricultural residue burning, brick production, cooking and heating are respectively 0.026 (± 0.035), 0.015 (± 0.026), 0.015 (± 0.003), and 0.010 (± 0.006) (Figure 3b). In agricultural residue burning, banana residue shows the lowest $k_{BrC,550}$ (0.008), and BC/OA ratio (0.030). In contrast, pigeon pea residue burning has the highest $k_{BrC,550}$ (0.082)
255 and BC/OA ratio (2.054). A similar relationship has also been observed in other source-fuel combinations and used to parameterize $k_{BrC,550}$ and w (Figure 4). The large variation in $k_{BrC,550}$

during agricultural residue burning could be due to differences in the combustion conditions and fuel properties (Holder et al., 2017; Chakrabarty et al., 2016; Nguyen et al., 1994), where banana, with a high moisture content (Tock et al., 2010), has a $k_{BrC,550}$ of 0.008 and pigeon pea (an oil seed legume) has a $k_{BrC,550}$ of 0.082. In comparison, $k_{BrC,550}$ varies from 0.006 (final-stage) to 0.022 (initial stage) during brick kiln operation and from 0.002 (crop residue) to 0.013 (firewood) during residential heating. The combustion conditions during these three activities are comparatively different could be because of the very low fuel feed rate. This contrasts with cooking, where deliberate efforts are made to ensure efficient burning of fuel for meal preparation. Hence, BrC properties in cooking emissions do not vary much ($k_{BrC,550}$= 0.015±0.001). Our study observed $k_{BrC,365}$ of ~0.1 (±0.01) for cooking, which is higher than lab-measured values (0.014-0.054) for the same fuels at 350 nm (Rathod et al., 2017). We observed that the $MAC_{BrC,365}$ stayed between 1.5-2.5 m^2 g^{-1} for all the source-fuel combinations, except for pigeon pea residue burning ($MAC_{BrC,365}$=4.01 m^2 g^{-1}). The current findings are comparable with the $MAC_{BrC,365}$ value of 2 (±0.5) m^2 g^{-1} from Indian airmasses influenced by agricultural residue burning (Satish et al., 2020). The values reported in our study are in the upper range of ambient $MAC_{BrC,365}$ (0.62-2.3) reported previously over India (Sarkar et al., 2019; Shamjad et al., 2018; Satish et al., 2020; Rastogi et al., 2021; Rana et al., 2020; Kirillova et al., 2016; Dey et al., 2021). The observed AAE_{BrC} (~5.23 ± 1.51, range 2-8.5, see Table S1) is comparable with previous observations (~5.31 ± 1.67, range 2.3-6.8) for biomass burning over India (Islam et al., 2022; Pandey et al., 2020; Rathod et al., 2017; Satish et al., 2020).
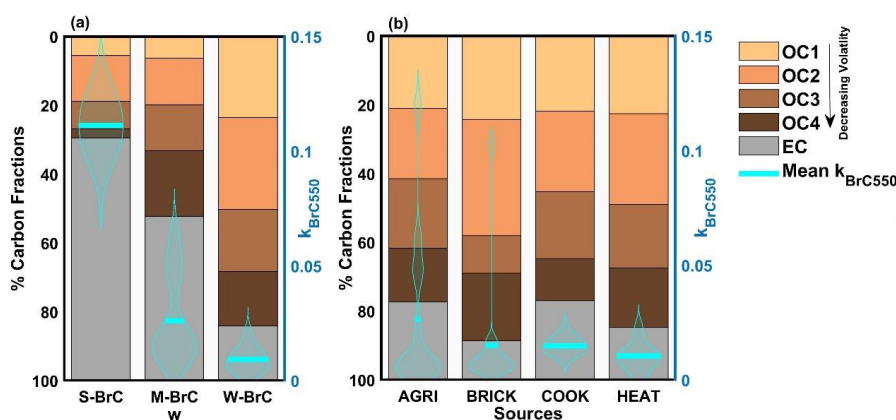
Figure 3. (a) $k_{BrC,50}$ distribution (right) and thermo-optically resolved carbon fractions (left) with varying BrC classes based on wavelength dependence. Here, the strongly absorbing BrC (S-BrC), moderately absorbing BrC (M-BrC) and weakly absorbing BrC (W-BrC) ranges are respectively <1.5, 1.5 - 4, and 4< in wavelength dependence (Saleh, 2020). **(b)** source specific $k_{BrC,550}$ distribution (right) and thermo-optically resolved carbon fractions (left). The distribution of violin plot shows the Kernel density. Arrow near legends indicates reduction in the relative volatility from OC1 to OC4 (Ma et al., 2016).

3.3. Parameterization of k_{BrC} and w

We leveraged the significant correlation (p-value < 0.01) between the BC to OA ratio and the BrC properties ($k_{BrC,550}$, R^2=0.93; w, R^2 = 0.60) to build a relationship between these quantities. Despite the variety of fuel burning technologies used, such as traditional stoves, open residue
290   burning, and brick clamps, $k_{BrC,550}$ variability is explained (R^2 = 0.93) by the BC to OA ratio. We observed that $k_{BrC,550}$ varies linearly from 0.006 to 0.74 for BC to OA ratios of 0 to 20 (Figure 4a). Similarly, we explain w by using the BC to OA ratio to provide an approximation of the BrC absorption over the different wavelengths. We observed an exponential relation between w and the BC to OA ratio with an R^2 of 0.60 (w varies from 5 to ~0 for BC to OA
295   ratios of 0 to 20, respectively) (Figure 4b). Relative to the present studies, the relationship used in climate modelling studies (Zhang et al., 2020; Neyestani and Saleh, 2022; Brown et al., 2018) given by Saleh et al. (2014) would overestimate the $k_{BrC,550}$ over South Asia (Figure S7). In contrast, previous studies (Saleh et al., 2014; Lu et al., 2015; Luo et al., 2022) underestimate the range of w observed in this study, which may result in an underestimation of $k_{BrC,365}$ (Figure
300   S7). Such an underestimation would propagate uncertainties to radiative forcing calculations, especially over South Asia.
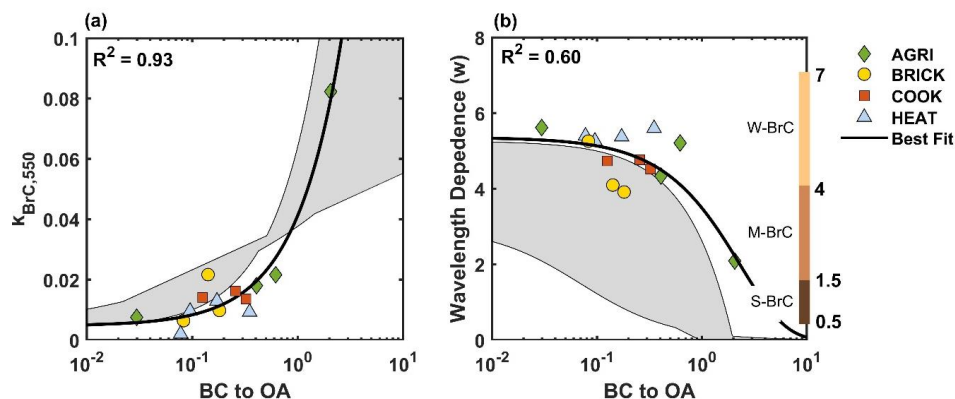
Figure 4. (a) Mean $K_{BrC,550}$ versus BC to OA ratio ($k_{BrC,550}$= 0.0365(±0.006)×(BC/OA)+0.0047(±0.0037), R^2=0.93) and **(b)** w versus the BC to OA ratio
305   (w=5.355(±0.50)×exp(-0.428(±0.25)×(BC/OA)), R^2=0.60). Here, OA = OC x 1.8: the factor 1.8 is widely used to convert OC into OA (Turpin et al., 2001; Chow et al., 2015; Navinya et al., 2020; Provençal et al., 2017; Kumar et al., 2023). The grey shaded area represents the relationship reported by previous studies (Saleh et al., 2014; Lu et al., 2015; Luo et al., 2022), and the equations for the shaded area are given in the supplementary information (S2, S3 and
310   figure S1). The right axis in Figure 4b displays the ranges of wavelength dependence for the three BrC classes.

3.4. Spatial Differences in $k_{BrC,365}$ and w

Several studies have reported ambient BrC absorption in the South Asian region (Dey et al.,
315   2023; Srinivas and Sarin, 2013, 2014; Bikkina et al., 2020; Boreddy et al., 2021; Choudhary et al., 2017, 2018, 2022; Dasari et al., 2019; Dey et al., 2021; Kirillova et al., 2016; Mukherjee et

al., 2020; Rajeev et al., 2022; Rastogi et al., 2021; Rana et al., 2020; Shamjad et al., 2016b, 2018), most climate models continue to consider weakly absorbing BrC absorption (Sand et al., 2021; Feng et al., 2013), invariant of sources and combustion conditions. Feng et al. (2013)
320 simulated global BrC absorption by using 2- to 5-fold weaker k_{BrC} values than those observed in our study, and they noted underestimation over South Asia owing to presence of strongly absorbing BrC. Other studies (Brown et al., 2018; Zhang et al., 2020) have used 2- to 3-fold higher $k_{BrC,550}$ values (Saleh et al., 2014; Mcmeeking, 2008) than observed in this study to simulate the global radiative impact of BrC. Hence, neglecting the spatial variability of k_{BrC}
325 could lead to bias in understanding its radiative impact. Thus, we calculated emissions-weighted BrC optical properties across the Indian region to demonstrate their spatial heterogeneity in the region. The relationships shown in Figure 4 were used to make a spatial map of $k_{BrC,550}$, $k_{BrC,365}$, and w, with emission strength from the COALESCE SMoG-India emission inventory (Tibrewal et al., 2024). SMoG-India is a multi-sectoral, multi-pollutant data
330 set available at 5 km grid resolution, developed under the COALESCE network (Venkataraman et al., 2020), which also facilitated the collection of samples used in the present study.

Figure 1 shows the large OC emissions over the Indo-Gangetic Plain, with annual emissions ranging from 50-70 Mg y^{-1} pixel^{-1} (pixel size is 5×5 km), while other regions emit ~10-20 Mg y^{-1} pixel^{-1}. Emission weighted spatial information about w (range: 4.3 - 5.3) and $k_{BrC,550}$ (0.006
335 – 0.023) aids the estimation of $k_{BrC,365}$. Figure 5a shows $k_{BrC,365}$ ranges from 0.05 to 0.14, indicating strong absorption in the UV-visible wavelengths. The northern hilly region (at the Himalayan foothills) shows very large k_{BrC}, mainly due to emissions from the predominant space heating activity. A recent study highlighted the low photobleaching rate of BrC near Himalayan regions due to the low ambient temperatures (Choudhary et al., 2022). The
340 coincidence of dark BrC particle emissions in this study, along with their reported extended lifetimes, could result in snow darkening on deposition, along with accelerated snow and glacier melting. Figure S3 shows high k_{BrC} in the northwestern parts of India, the result of agricultural residue burning, while high k_{BrC} in East India is mainly associated with heating activities. The $k_{BrC,550}$ values of combustion aerosol emissions from India vary from 0.006 to
345 0.023 (Figure S6), with some hotspots scattered across the country. These numbers highlight the order of magnitude increase in $k_{BrC,365}$ compared to $k_{BrC,550}$, with higher values over Eastern and Northern India. An earlier investigation also noted elevated modelled BrC absorption in the Eastern regions of India (Zhu et al., 2021). With a higher abundance of OC, along with a high k_{BrC}, South Asia is more likely to see atmospheric persistence of BrC due to continuous
350 emissions of fresh BrC and the extended time required for photobleaching.
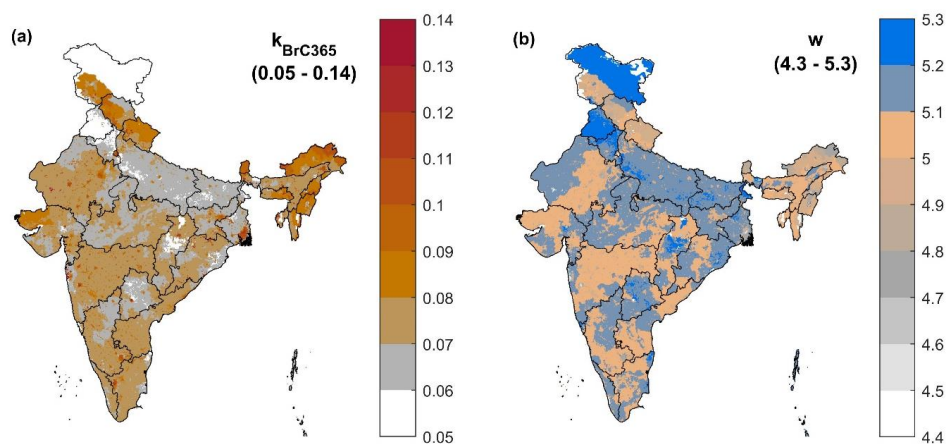
Figure 5. The spatial distribution of **(a)** $k_{BrC,365}$ and **(b)** wavelength dependence (w). The BC to OA ratio is taken for the year 2019 from the COALESCE SMoG-India emission inventory (Tibrewal et al., 2024).

355

4. Implications

The variability in $k_{BrC,near-UV}$ across modelling studies, ranging from 0.045 (Zhang et al., 2020) to 0.168 (Lin et al., 2014), arises from methodological, fuel, and burning condition disparities in the studies reporting BrC absorption properties from lab-based biomass combustion
360 (Kirchstetter et al., 2004; Chen and Bond, 2010; Lack et al., 2012). However, our study, by using field measurements of a variety of sources, introduces source- and fuel-specific k_{BrC} values, enhancing modelling capabilities for a more nuanced understanding of the radiative and climate impacts of BrC. Additionally, the observed varying wavelength dependence (w), linked with the BC to OA ratio in this research, amplifies uncertainty when it is assumed to be constant
365 in models (Zhang et al., 2020). Compared to the findings of this study, typical BrC parameterization schemes (Saleh et al., 2014; Lu et al., 2015; Luo et al., 2022) in climate models tend to overestimate $k_{BrC,550}$ while substantially underestimating wavelength dependence, which may misrepresent near-UV BrC absorption in world regions with biomass combustion emissions resembling those in South Asia. Additionally, this study's findings aid in
370 pinpointing biomass fuels and activities, including burning of some agricultural residues and residential space heating, that are both prone to emitting stronger absorbing BrC ($k_{BrC,550} > 0.1$) and prevalent across developing nations. These variations in k_{BrC} with sources and fuels lead to spatial variations in emitted BrC properties. In the Himalayan foothills, residential space heating produces stronger absorbing (and more persistent) BrC emissions, and the deposition
375 of these emissions increases the potential risks of increased snow darkening and accelerated glacier melting. Leveraging this information with emission inventories enables the identification and potential interventional targeting these biomass fuels and activities, towards reducing both their local health and global climate impacts.

380 **Acknowledgements**

The authors thank the Fulbright Program {Fulbright-Kalam Climate Fellowship Award No. 2913/FNDR/2023-2024 to CN} and the IIT Bombay – WashU program for financial support to conduct a part of this work at Washington University in St. Louis. This work was supported by the Indian Ministry of Environment Forest and Climate Change under the NCAP-

385 COALESCE project {Grant No.14/10/2014-CC(Vol.II)}. The views expressed in this document are solely those of authors and do not necessarily reflect those of the Ministry. The Ministry does not endorse any products or commercial services mentioned in this publication.

Data Availability

390 The data used in this study are provided in the supplementary information of the article.

Conflict of Interest

The authors declare that they have no conflict of interest.

395 **Author contributions**

Conceptualization: CV, RKC, CN, TSK; **Methodology, Formal Analysis:** RKC, CN, TSK; **Software, Visualization:** CN; **Data Curation:** CN, TSK, GA; **Writing - Original Draft:** CN; **Writing - Review & Editing:** TSK, RKC, CV, HCP, GA; **Supervision:** RKC, CV, HCP.

400

References

Arola, A., Schuster, G. L., Pitkänen, M. R. A., Dubovik, O., Kokkola, H., Lindfors, A. V., Mielonen, T., Raatikainen, T., Romakkaniemi, S., Tripathi, S. N., and Lihavainen, H.: Direct radiative effect by brown carbon over the Indo-Gangetic Plain, Atmos. Chem. Phys., 15, 12731–12740, https://doi.org/10.5194/acp-15-12731-2015, 2015.

Azhar, R., Zeeshan, M., and Fatima, K.: Crop residue open field burning in Pakistan; multi-year high spatial resolution emission inventory for 2000–2014, Atmos. Environ., 208, 20–33, https://doi.org/10.1016/J.ATMOSENV.2019.03.031, 2019.

Bhowmik, H. S., Tripathi, S. N., Shukla, A. K., Lalchandani, V., Murari, V., Devaprasad, M., Shivam, A., Bhushan, R., Prévôt, A. S. H., and Rastogi, N.: Contribution of fossil and biomass-derived secondary organic carbon to winter water-soluble organic aerosols in Delhi, India, Sci. Total Environ., 912, 168655, https://doi.org/10.1016/J.SCITOTENV.2023.168655, 2024.

Bikkina, P., Bikkina, S., Kawamura, K., Sudheer, A. K., Mahesh, G., and Kumar, S. K.: Evidence for brown carbon absorption over the Bay of Bengal during the southwest monsoon season: A possible oceanic source, Environ. Sci. Process. Impacts, 22, 1743–1758, https://doi.org/10.1039/d0em00111b, 2020.

Bikkina, S. and Sarin, M.: Brown carbon in the continental outflow to the North Indian Ocean, Environ. Sci. Process. Impacts, 21, 970–987, https://doi.org/10.1039/c9em00089e, 2019.

Bond, T. C. and Bergstrom, R. W.: Light absorption by carbonaceous particles: An investigative review, Aerosol Sci. Technol., 40, 27–67, https://doi.org/10.1080/02786820500421521, 2006.

Bond, T. C., Doherty, S. J., Fahey, D. W., Forster, P. M., Berntsen, T., Deangelo, B. J., Flanner, M. G., Ghan, S., Kärcher, B., Koch, D., Kinne, S., Kondo, Y., Quinn, P. K., Sarofim, M. C., Schultz, M. G., Schulz, M., Venkataraman, C., Zhang, H., Zhang, S., Bellouin, N., Guttikunda, S. K., Hopke, P. K., Jacobson, M. Z., Kaiser, J. W., Klimont, Z., Lohmann, U., Schwarz, J. P., Shindell, D., Storelvmo, T., Warren, S. G., and Zender, C. S.: Bounding the role of black carbon in the climate system: A scientific assessment, 118, 5380–5552, https://doi.org/10.1002/JGRD.50171, 2013.

Bonjour, S., Adair-Rohani, H., Wolf, J., Bruce, N. G., Mehta, S., Prüss-Ustün, A., Lahiff, M., Rehfuess, E. A., Mishra, V., and Smith, K. R.: Solid fuel use for household cooking: Country and regional estimates for 1980-2010, Environ. Health Perspect., 121, 784–790, https://doi.org/10.1289/EHP.1205987/SUPPL_FILE/EHP.1205987.S001.PDF, 2013.

Boreddy, S. K. R., Hegde, P., Aswini, A. R., and Aryasree, S.: Chemical Characteristics, Size Distributions, Molecular Composition, and Brown Carbon in South Asian Outflow to the Indian Ocean, Earth Sp. Sci., 8, 1–32, https://doi.org/10.1029/2020EA001615, 2021.

Brown, H., Liu, X., Feng, Y., Jiang, Y., Wu, M., Lu, Z., Wu, C., Murphy, S., and Pokhrel, R.: Radiative effect and climate impacts of brown carbon with the Community Atmosphere Model (CAM5), Atmos. Chem. Phys., 18, 17745–17768, https://doi.org/10.5194/acp-18-17745-2018, 2018.

Chakrabarty, R. K., Moosmüller, H., Chen, L. W. A., Lewis, K., Arnott, W. P., Mazzoleni, C., Dubey, M. K., Wold, C. E., Hao, W. M., and Kreidenweis, S. M.: Brown carbon in tar balls from smoldering biomass combustion, Atmos. Chem. Phys., 10, 6363–6370,

445   https://doi.org/10.5194/ACP-10-6363-2010, 2010.

Chakrabarty, R. K., Gyawali, M., Yatavelli, R. L. N., Pandey, A., Watts, A. C., Knue, J., Chen, L.-W. A., Pattison, R. R., Tsibart, A., Samburova, V., and Moosmüller, H.: Brown carbon aerosols from burning of boreal peatlands: microphysical properties, emission factors, and implications for direct radiative forcing, Atmos. Chem. Phys., 16, 3033–3040,
450   https://doi.org/10.5194/acp-16-3033-2016, 2016.

Chakrabarty, R. K., Shetty, N. J., Thind, A. S., Beeler, P., Sumlin, B. J., Zhang, C., Liu, P., Idrobo, J. C., Adachi, K., Wagner, N. L., Schwarz, J. P., Ahern, A., Sedlacek, A. J., Lambe, A., Daube, C., Lyu, M., Liu, C., Herndon, S., Onasch, T. B., and Mishra, R.: Shortwave absorption by wildfire smoke dominated by dark brown carbon, Nat. Geosci., 16, 683–688,
455   https://doi.org/10.1038/s41561-023-01237-9, 2023.

Chen, L. W. A., Chow, J. C., Wang, X., Cao, J., Mao, J., and Watson, J. G.: Brownness of Organic Aerosol over the United States: Evidence for Seasonal Biomass Burning and Photobleaching Effects, Environ. Sci. Technol., 55, 8561–8572, https://doi.org/10.1021/ACS.EST.0C08706/SUPPL_FILE/ES0C08706_SI_002.XLSX, 2021.

460   Chen, Y. and Bond, T. C.: Light absorption by organic carbon from wood combustion, Atmos. Chem. Phys., 10, 1773–1787, https://doi.org/10.5194/ACP-10-1773-2010, 2010.

Cheng, Z., Atwi, K., Hajj, O. El, Ijeli, I., Fischer, D. Al, Smith, G., and Saleh, R.: Discrepancies between brown carbon light-absorption properties retrieved from online and offline measurements, Aerosol Sci. Technol., 55, 92–103,
465   https://doi.org/10.1080/02786826.2020.1820940, 2021.

Choudhary, V., Rajput, P., Rajeev, P., and Gupta, T.: Synergistic effect in absorption properties of brown carbon and elemental carbon over IGP during weak south-west monsoon, Aerosol Sci. Eng., 1, 138–149, https://doi.org/10.1007/s41810-017-0013-1, 2017.

Choudhary, V., Rajput, P., Singh, D. K., Singh, A. K., and Gupta, T.: Light absorption
470   characteristics of brown carbon during foggy and non-foggy episodes over the Indo-Gangetic Plain, Atmos. Pollut. Res., 9, 494–501, https://doi.org/10.1016/j.apr.2017.11.012, 2018.

Choudhary, V., Singh, G. K., Gupta, T., and Paul, D.: Absorption and radiative characteristics of brown carbon aerosols during crop residue burning in the source region of Indo-Gangetic Plain, Atmos. Res., 249, 105285,
475   https://doi.org/10.1016/j.atmosres.2020.105285, 2021.

Choudhary, V., Gupta, T., and Zhao, R.: Evolution of Brown Carbon Aerosols during Atmospheric Long-Range Transport in the South Asian Outflow and Himalayan Cryosphere, ACS Earth Sp. Chem., 6, 2335–2347, https://doi.org/10.1021/acsearthspacechem.2c00047, 2022.

480   Chow, J. C., Watson, J. G., Chen, L. W. A., Chang, M. C. O., Robinson, N. F., Trimble, D., and Kohl, S.: The IMPROVE_A Temperature Protocol for Thermal/Optical Carbon Analysis: Maintaining Consistency with a Long-Term Database, J. Air Waste Manage. Assoc., 57, 1014–1023, https://doi.org/10.3155/1047-3289.57.9.1014, 2007.

Chow, J. C., Lowenthal, D. H., Chen, L. W. A., Wang, X., and Watson, J. G.: Mass
485   reconstruction methods for PM2.5: a review, Air Qual. Atmos. Heal., 8, 243–263, https://doi.org/10.1007/s11869-015-0338-3, 2015.

Corbin, J. C., Czech, H., Massabò, D., de Mongeot, F. B., Jakobi, G., Liu, F., Lobo, P.,

Mennucci, C., Mensah, A. A., Orasche, J., Pieber, S. M., Prévôt, A. S. H., Stengel, B., Tay, L. L., Zanatta, M., Zimmermann, R., El Haddad, I., and Gysel, M.: Infrared-absorbing
490   carbonaceous tar can dominate light absorption by marine-engine exhaust, npj Clim. Atmos. Sci. 2019 21, 2, 1–10, https://doi.org/10.1038/s41612-019-0069-5, 2019.

Crippa, M., Guizzardi, D., Muntean, M., Schaaf, E., Dentener, F., Van Aardenne, J. A., Monni, S., Doering, U., Olivier, J. G. J., Pagliari, V., and Janssens-Maenhout, G.: Gridded emissions of air pollutants for the period 1970-2012 within EDGAR v4.3.2, Earth Syst. Sci.
495   Data, 10, 1987–2013, https://doi.org/10.5194/ESSD-10-1987-2018, 2018.

Dasari, S., Andersson, A., Bikkina, S., Holmstrand, H., Budhavant, K., Satheesh, S., Asmi, E., Kesti, J., Backman, J., Salam, A., Bisht, D. S., Tiwari, S., Hameed, Z., and Gustafsson, Ö.: Photochemical degradation affects the light absorption of water-soluble brown carbon in the South Asian outflow, Sci. Adv., 5, 1–11, https://doi.org/10.1126/sciadv.aau8066, 2019.

500   Devaprasad, M., Rastogi, N., Satish, R., Patel, A., Dabhi, A., Shivam, A., Bhushan, R., and Meena, R.: Dual carbon isotope-based brown carbon aerosol characteristics at a high-altitude site in the northeastern Himalayas: Role of biomass burning, Sci. Total Environ., 912, 169451, https://doi.org/10.1016/J.SCITOTENV.2023.169451, 2024.

Dey, S., Mukherjee, A., Polana, A. J., Rana, A., Mao, J., Jia, S., Yadav, A. K., Khillare, P. S.,
505   and Sarkar, S.: Brown carbon aerosols in the Indo-Gangetic Plain outflow: Insights from excitation emission matrix (EEM) fluorescence spectroscopy, Environ. Sci. Process. Impacts, 23, 745–755, https://doi.org/10.1039/d1em00050k, 2021.

Dey, S., Ghosh, P., Rawat, P., Choudhary, N., Rai, A., Meena, R., Mandal, T. K., Mao, J., Jia, S., Rastogi, N., Sharma, S. K., and Sarkar, S.: Optical source apportionment of aqueous
510   brown carbon (BrC) on a daytime and nighttime basis in the eastern Indo-Gangetic Plain (IGP) and insights from 13C and 15N isotopic signatures, Sci. Total Environ., 894, 164872, https://doi.org/10.1016/j.scitotenv.2023.164872, 2023.

DRI Manual: DRI Model 2015 Multiwavelength Thermal/Optical Carbon Analyzer Installation, Operation, and Service Manual, 2015, 2015.

515   Feng, Y., Ramanathan, V., and Kotamarthi, V. R.: Brown carbon: A significant atmospheric absorber of solar radiation, Atmos. Chem. Phys., 13, 8607–8621, https://doi.org/10.5194/acp-13-8607-2013, 2013.

Gliß, J., Mortier, A., Schulz, M., Andrews, E., Balkanski, Y., Bauer, S. E., Benedictow, A. M. K., Bian, H., Checa-Garcia, R., Chin, M., Ginoux, P., Griesfeller, J. J., Heckel, A.,
520   Kipling, Z., Kirkeväg, A., Kokkola, H., Laj, P., Le Sager, P., Tronstad Lund, M., Lund Myhre, C., Matsui, H., Myhre, G., Neubauer, D., Van Noije, T., North, P., Olivié, D. J. L., Rémy, S., Sogacheva, L., Takemura, T., Tsigaridis, K., and Tsyro, S. G.: AeroCom phase III multi-model evaluation of the aerosol life cycle and optical properties using ground- And space-based remote sensing as well as surface in situ observations, Atmos. Chem. Phys., 21,
525   87–128, https://doi.org/10.5194/ACP-21-87-2021, 2021.

Gyawali, M., Arnott, W. P., Zaveri, R. A., Song, C., Pekour, M., Flowers, B., Dubey, M. K., Setyan, A., Zhang, Q., Harworth, J. W., Radney, J. G., Atkinson, D. B., China, S., Mazzoleni, C., Gorkowski, K., Subramanian, R., Jobson, B. T., Moosmüller, H., and Moosmüller, M.: Evolution of multispectral aerosol optical properties in a biogenically-influenced urban
530   environment during the CARES campaign, acp.copernicus.orgM Gyawali, WP Arnott, RA Zaveri, C Song, M Pekour, B Flowers, MK Dubey, A SetyanAtmospheric Chem. Phys. Discuss. 2013•acp.copernicus.org, 13, 7113–7150, https://doi.org/10.5194/acpd-13-7113-

2013, 2013.

535 Habib, G., Kumari, J., Khan, M., Zaidi, K., Yogesh, A., Nagendra, S. M. S., Navinya, C., Phuleria, H., Bombay, I., Arya, R., Mandal, T., Delhi, N., Muthalagu, A., Qureshi, A., Bhat, R., and Jehangir, A.: Estimating shifts in fuel stacking among solid biomass fuels and liquified petroleum gas in rural households: A pan-India analysis, Prepr. Res. Sq., 2023.

Hecobian, A., Zhang, X., Zheng, M., Frank, N., Edgerton, E. S., and Weber, R. J.: Water-soluble organic aerosol material and the light-absorption characteristics of aqueous extracts measured over the Southeastern United States, Atmos. Chem. Phys., 10, 5965–5977, https://doi.org/10.5194/ACP-10-5965-2010, 2010.

Holder, A. L., Gullett, B. K., Urbanski, S. P., Elleman, R., O'Neill, S., Tabor, D., Mitchell, W., and Baker, K. R.: Emissions from prescribed burning of agricultural fields in the Pacific Northwest, Atmos. Environ., 166, 22–33, 545 https://doi.org/10.1016/J.ATMOSENV.2017.06.043, 2017.

Islam, M. M., Neyestani, S. E., Saleh, R., and Grieshop, A. P.: Quantifying brown carbon light absorption in real-world biofuel combustion emissions, Aerosol Sci. Technol., 56, 502–516, https://doi.org/10.1080/02786826.2022.2051425, 2022.

Jennings, S. G., Pinnick, R. G., and Gillespie, J. B.: Relation between absorption coefficient 550 and imaginary index of atmospheric aerosol constituents, Appl. Opt., 18, 1368, https://doi.org/10.1364/ao.18.001368, 1979.

Kapoor, T. S., Venkataraman, C., Sarkar, C., Phuleria, H. C., Chatterjee, A., Habib, G., and Apte, J. S.: Estimation of real-time brown carbon absorption: An observationally constrained Mie theory-based optimization method, J. Aerosol Sci., 106047, 555 https://doi.org/10.1016/J.JAEROSCI.2022.106047, 2022.

Kapoor, T. S., Phuleria, H. C., Sumlin, B., Shetty, N., Anurag, G., Bansal, M., Duhan, S. S., Khan, M. S., Laura, J. S., Manwani, P., Chakrabarty, R. K., and Venkataraman, C.: Optical Properties and Refractive Index of Wintertime Aerosol at a Highly Polluted North-Indian Site, J. Geophys. Res. Atmos., 128, 1–14, https://doi.org/10.1029/2022JD038272, 2023a.

560 Kapoor, T. S., Navinya, C., Anurag, G., Lokhande, P., Rathi, S., Goel, A., Sharma, R., Arya, R., Mandal, T. K., Jithin, K. P., Nagendra, S., Imran, M., Kumari, J., Muthalagu, A., Qureshi, A., Najar, T. A., Jehangir, A., Haswani, D., Raman, R. S., Rabha, S., Saikia, B., Lian, Y., Pandithurai, G., Chaudhary, P., Sinha, B., Dhandapani, A., Iqbal, J., Mukherjee, S., Chatterjee, A., Venkataraman, C., and Phuleria, H. C.: Reassessing the availability of crop 565 residue as a bioenergy resource in India: A field-survey based study, J. Environ. Manage., 341, 118055, https://doi.org/10.1016/j.jenvman.2023.118055, 2023b.

Kirchstetter, T. W., Novakov, T., and Hobbs, P. V.: Evidence that the spectral dependence of light absorption by aerosols is affected by organic carbon, J. Geophys. Res. D Atmos., 109, 1–12, https://doi.org/10.1029/2004JD004999, 2004.

570 Kirillova, E. N., Marinoni, A., Bonasoni, P., Vuillermoz, E., Facchini, M. C., Fuzzi, S., and Decesari, S.: Light absorption properties of brown carbon in the high Himalayas, J. Geophys. Res., 121, 9621–9639, https://doi.org/10.1002/2016JD025030, 2016.

Kroll, J. H. and Seinfeld, J. H.: Chemistry of secondary organic aerosol: Formation and evolution of low-volatility organics in the atmosphere, Atmos. Environ., 42, 3593–3624, 575 https://doi.org/10.1016/J.ATMOSENV.2008.01.003, 2008.

Kroll, J. H., Chan, A. W. H., Ng, N. L., Flagan, R. C., and Seinfeld, J. H.: Reactions of semivolatile organics and their effects on secondary organic aerosol formation, Environ. Sci. Technol., 41, 3545–3550, https://doi.org/10.1021/ES062059X/ASSET/IMAGES/LARGE/ES062059XF00004.JPEG, 2007.

580

Kumar, V., Malyan, V., Sahu, M., Biswal, B., Pawar, M., and Dev, I.: Spatiotemporal analysis of fine particulate matter for India (1980–2021) from MERRA-2 using ensemble machine learning, Atmos. Pollut. Res., 14, 101834, https://doi.org/10.1016/J.APR.2023.101834, 2023.

585   Kumari, J., Jain, K., Zaidi, K., and Habib, G.: Design and evaluation of a new source sampler for on-field emission measurement from combustion sources, in: AAAR 39th Annual Virtual Conference, https://doi.org/https://aaarabstracts.com/2021/AbstractBook.pdf, 2021.

Kurokawa, J. and Ohara, T.: Long-term historical trends in air pollutant emissions in Asia: Regional Emission inventory in ASia (REAS) version 3, Atmos. Chem. Phys., 20, 12761–
590   12793, https://doi.org/10.5194/ACP-20-12761-2020, 2020.

Lack, D. A., Langridge, J. M., Bahreini, R., Cappa, C. D., Middlebrook, A. M., and Schwarz, J. P.: Brown carbon and internal mixing in biomass burning particles, Proc. Natl. Acad. Sci. U. S. A., 109, 14802–14807, https://doi.org/10.1073/PNAS.1206575109/-/DCSUPPLEMENTAL/PNAS.1206575109_SI.PDF, 2012.

595   Lee, J., Kim, J., Song, C. H., Kim, S. B., Chun, Y., Sohn, B. J., and Holben, B. N.: Characteristics of aerosol types from AERONET sunphotometer measurements, Atmos. Environ., 44, 3110–3117, https://doi.org/10.1016/J.ATMOSENV.2010.05.035, 2010.

Lin, G., Penner, J. E., Flanner, M. G., Sillman, S., Xu, L., and Zhou, C.: Radiative forcing of organic aerosol in the atmosphere and on snow: Effects of SOA and brown carbon, J.
600   Geophys. Res., 119, 7453–7476, https://doi.org/10.1002/2013JD021186, 2014.

Liu, C., Chung, C. E., Yin, Y., and Schnaiter, M.: The absorption Ångström exponent of black carbon: from numerical aspects, acp.copernicus.org, 18, 6259–6273, https://doi.org/10.5194/acp-18-6259-2018, 2018.

Liu, J., Bergin, M., Guo, H., King, L., Kotra, N., Edgerton, E., and Weber, R. J.: Size-
605   resolved measurements of brown carbon in water and methanol extracts and estimates of their contribution to ambient fine-particle light absorption, Atmos. Chem. Phys., 13, 12389–12404, https://doi.org/10.5194/ACP-13-12389-2013, 2013.

Lu, Z., Streets, D. G., Winijkul, E., Yan, F., Chen, Y., Bond, T. C., Feng, Y., Dubey, M. K., Liu, S., Pinto, J. P., and Carmichael, G. R.: Light absorption properties and radiative effects
610   of primary organic aerosol emissions, Environ. Sci. Technol., 49, 4868–4877, https://doi.org/10.1021/ACS.EST.5B00211/SUPPL_FILE/ES5B00211_SI_001.PDF, 2015.

Luo, B., Kuang, Y., Huang, S., Song, Q., Hu, W., Li, W., Peng, Y., Chen, D., Yue, D., Yuan, B., and Shao, M.: Parameterizations of size distribution and refractive index of biomass burning organic aerosol with black carbon content, Atmos. Chem. Phys., 22, 12401–12415,
615   https://doi.org/10.5194/ACP-22-12401-2022, 2022.

Ma, J., Li, X., Gu, P., Dallmann, T. R., Presto, A. A., and Donahue, N. M.: Estimating ambient particulate organic carbon concentrations and partitioning using thermal optical measurements and the volatility basis set, Aerosol Sci. Technol., 50, 638–651, https://doi.org/10.1080/02786826.2016.1158778, 2016.

620   Mcduffie, E. E., Smith, S. J., O'rourke, P., Tibrewal, K., Venkataraman, C., Marais, E. A., Zheng, B., Crippa, M., Brauer, M., and Martin, R. V: A global anthropogenic emission inventory of atmospheric pollutants from sector-and fuel-specific sources (1970-2017): an application of the Community Emissions Data System (CEDS), Earth Syst. Sci. Data, 12, 3413–3442, https://doi.org/10.5194/essd-12-3413-2020, 2020.

625   Mcmeeking, G. R.: DISSERTATION THE OPTICAL, CHEMICAL, AND PHYSICAL PROPERTIES OF AEROSOLS AND GASES EMITTED BY THE LABORATORY COMBUSTION OF WILDLAND FUELS Submitted by, 2008.

Mukherjee, A., Dey, S., Rana, A., Jia, S., Banerjee, S., and Sarkar, S.: Sources and atmospheric processing of brown carbon and HULIS in the Indo-Gangetic Plain: Insights
630   from compositional analysis, Environ. Pollut., 267, 115440, https://doi.org/10.1016/j.envpol.2020.115440, 2020.

Navinya, C., Kapoor, T. S., Gupta, A. K., Lokhande, P., Sharma, R., SV, L. P., SM, S. N., Kumari, J., Habib, G., Arya, R., Mandal, T. K., Muthalagu, A., Qureshi, A., Najar, T. A., Jehangir, A., Jain, S., Goel, A., Rabha, S., Saikia, B., Chaudhary, P., Sinha, B., Haswani, D.,
635   Raman, R. S., Dhandapani, A., Iqbal, J., Mukherjee, S., Chatterjee, A., Lian, Y., Pandithurai, G., Venkataraman, C., and Phuleria, H. C.: Heating and lighting: Understanding overlooked energy-consumption activities in the Indian residential sector, Environ. Res. Commun., https://doi.org/10.1088/2515-7620/ACCA6F, 2023.

Navinya, C. D., Vinoj, V., and Pandey, S. K.: Evaluation of pm2.5 surface concentrations
640   simulated by nasa's merra version 2 aerosol reanalysis over india and its relation to the air quality index, Aerosol Air Qual. Res., 20, 1329–1339, https://doi.org/10.4209/aaqr.2019.12.0615, 2020.

Neyestani, S. E. and Saleh, R.: Observationally constrained representation of brown carbon emissions from wildfires in a chemical transport model, Environ. Sci. Atmos., 2, 192–201,
645   https://doi.org/10.1039/D1EA00059D, 2022.

Nguyen, B. C., Putaud, J. P., Mihalopoulos, N., Bonsang, B., and Doan, C.: CH4 and CO emissions from rice straw burning in South East Asia, Environ. Monit. Assess., 31, 131–137, https://doi.org/10.1007/BF00547188, 1994.

Ohara, T., Akimoto, H., Kurokawa, J., Horii, N., Yamaji, K., Yan, X., and Hayasaka, T.: An
650   Asian emission inventory of anthropogenic emission sources for the period 1980-2020, Atmos. Chem. Phys., 7, 4419–4444, https://doi.org/10.5194/ACP-7-4419-2007, 2007.

Pandey, A., Sadavarte, P., Rao, A. B., and Venkataraman, C.: Trends in multi-pollutant emissions from a technology-linked inventory for India: II. Residential, agricultural and informal industry sectors, Atmos. Environ., 99, 341–352,
655   https://doi.org/10.1016/j.atmosenv.2014.09.080, 2014.

Pandey, A., Hsu, A., Tiwari, S., Pervez, S., and Chakrabarty, R. K.: Light Absorption by Organic Aerosol Emissions Rivals That of Black Carbon from Residential Biomass Fuels in South Asia, Environ. Sci. Technol. Lett., 7, 266–272, https://doi.org/10.1021/acs.estlett.0c00058, 2020.

660   Park, R. J., Kim, M. J., Jeong, J. I., Youn, D., and Kim, S.: A contribution of brown carbon aerosol to the aerosol light absorption and its radiative forcing in East Asia, Atmos. Environ., 44, 1414–1421, https://doi.org/10.1016/J.ATMOSENV.2010.01.042, 2010.

Provençal, S., Buchard, V., da Silva, A. M., Leduc, R., Barrette, N., Elhacham, E., and Wang,

S. H.: Evaluation of PM2.5 surface concentrations simulated by version 1 of NASA's
665   MERRA aerosol reanalysis over Israel and Taiwan, Aerosol Air Qual. Res., 17, 253–261,
https://doi.org/10.4209/aaqr.2016.04.0145, 2017.

Rajeev, P., Choudhary, V., Chakraborty, A., and Kumar, G.: Light absorption potential of
water-soluble organic aerosols in the two polluted urban locations in the central Indo-
Gangetic Plain ☆, Environ. Pollut., 314, 120228,
670   https://doi.org/10.1016/j.envpol.2022.120228, 2022.

Rana, A., Dey, S., Rawat, P., Mukherjee, A., Mao, J., Jia, S., Khillare, P. S., Yadav, A. K.,
and Sarkar, S.: Optical properties of aerosol brown carbon (BrC) in the eastern Indo-Gangetic
Plain, Sci. Total Environ., 716, 137102, https://doi.org/10.1016/j.scitotenv.2020.137102,
2020.

675   Rastogi, N., Satish, R., Singh, A., Kumar, V., Thamban, N., Lalchandani, V., Shukla, A.,
Vats, P., Tripathi, S. N., Ganguly, D., Slowik, J., and Prevot, A. S. H.: Diurnal variability in
the spectral characteristics and sources of water-soluble brown carbon aerosols over Delhi,
Sci. Total Environ., 794, 148589, https://doi.org/10.1016/j.scitotenv.2021.148589, 2021.

Rathod, T., Sahu, S. K., Tiwari, M., Yousaf, A., Bhangare, R. C., and Pandit, G. G.: Light
680   absorbing properties of brown carbon generated from pyrolytic combustion of household
biofuels, Aerosol Air Qual. Res., 17, 108–116, https://doi.org/10.4209/aaqr.2015.11.0639,
2017.

Roden, C. A., Bond, T. C., Conway, S., and Osorto Pinel, A. B.: Emission factors and real-
time optical properties of particles emitted from traditional wood burning cookstoves,
685   Environ. Sci. Technol., 40, 6750–6757, https://doi.org/10.1021/es052080i, 2006.

Romonosky, D. E., Ali, N. N., Saiduddin, M. N., Wu, M., Lee, H. J. J., Aiona, P. K., and
Nizkorodov, S. A.: Effective absorption cross sections and photolysis rates of anthropogenic
and biogenic secondary organic aerosols, Atmos. Environ., 130, 172–179,
https://doi.org/10.1016/J.ATMOSENV.2015.10.019, 2016.

690   Roy, S., Lam, Y. F., Hoque, M. M., and Chopra, S. S.: Review of Decadal Changes in
ASEAN Emissions Based on Regional and Global Emission Inventory Datasets, Aerosol Air
Qual. Res., 23, 220103, https://doi.org/10.4209/AAQR.220103, 2023.

Sadavarte, P., Rupakheti, M., Bhave, P., Shakya, K., and Lawrence, M.: Nepal emission
inventory - Part I: Technologies and combustion sources (NEEMI-Tech) for 2001-2016,
695   Atmos. Chem. Phys., 19, 12953–12973, https://doi.org/10.5194/acp-2019-113, 2019.

Saleh, R.: From Measurements to Models: Toward Accurate Representation of Brown
Carbon in Climate Calculations, Curr. Pollut. Reports, 6, 90–104,
https://doi.org/10.1007/s40726-020-00139-3, 2020.

Saleh, R., Robinson, E. S., Tkacik, D. S., Ahern, A. T., Liu, S., Aiken, A. C., Sullivan, R. C.,
700   Presto, A. A., Dubey, M. K., Yokelson, R. J., Donahue, N. M., and Robinson, A. L.:
Brownness of organics in aerosols from biomass burning linked to their black carbon content,
https://doi.org/10.1038/NGEO2220, 2014.

Saleh, R., Cheng, Z., and Atwi, K.: The Brown-Black Continuum of Light-Absorbing
Combustion Aerosols, Environ. Sci. Technol. Lett., 5, 508–513,
705   https://doi.org/10.1021/acs.estlett.8b00305, 2018.

Sand, M., Samset, B. H., Myhre, G., Gliß, J., Bauer, S. E., Bian, H., Chin, M., Checa-Garcia,

R., Ginoux, P., Kipling, Z., Kirkeväg, A., Kokkola, H., Le Sager, P., Lund, M. T., Matsui, H., Van Noije, T., Olivié, D. J. L., Remy, S., Schulz, M., Stier, P., Stjern, C. W., Takemura, T., Tsigaridis, K., Tsyro, S. G., and Watson-Parris, D.: Aerosol absorption in global models from
710   AeroCom phase III, Atmos. Chem. Phys., 21, 15929–15947, https://doi.org/10.5194/ACP-21-15929-2021, 2021.

Sarkar, C., Venkataraman, C., Yadav, S., Phuleria, H. C., and Chatterjee, A.: Origin and properties of soluble brown carbon in freshly emitted and aged ambient aerosols over an urban site in India, Environ. Pollut., 254, 113077,
715   https://doi.org/10.1016/j.envpol.2019.113077, 2019.

Satish, R. and Rastogi, N.: On the Use of Brown Carbon Spectra as a Tool to Understand Their Broader Composition and Characteristics: A Case Study from Crop-residue Burning Samples, ACS Omega, 4, 1814–1853, https://doi.org/10.1021/acsomega.8b02637, 2019.

Satish, R., Rastogi, N., Singh, A., and Singh, D.: Change in characteristics of water-soluble
720   and water-insoluble brown carbon aerosols during a large-scale biomass burning, Environ. Sci. Pollut. Res., 27, 33339–33350, https://doi.org/10.1007/s11356-020-09388-7, 2020.

Shamjad, P. M., Tripathi, S. N., Thamban, N. M., and Vreeland, H.: Refractive index and absorption attribution of highly absorbing brown carbon aerosols from an urban Indian city-Kanpur, Sci. Rep., 6, https://doi.org/10.1038/SREP37735, 2016a.

725   Shamjad, P. M., Tripathi, S. N., Thamban, N. M., and Vreeland, H.: Refractive Index and Absorption Attribution of Highly Absorbing Brown Carbon Aerosols from an Urban Indian City-Kanpur OPEN, https://doi.org/10.1038/srep37735, 2016b.

Shamjad, P. M., Satish, R. V., Thamban, N. M., Rastogi, N., and Tripathi, S. N.: Absorbing Refractive Index and Direct Radiative Forcing of Atmospheric Brown Carbon over Gangetic
730   Plain, ACS Earth Sp. Chem., 2, 31–37, https://doi.org/10.1021/acsearthspacechem.7b00074, 2018.

Shetty, N., Liu, P., Liang, Y., Sumlin, B., Daube, C., Herndon, S., Goldstein, A. H., and Chakrabarty, R. K.: Brown carbon absorptivity in fresh wildfire smoke: associations with volatility and chemical compound groups, Environ. Sci. Atmos., 3, 1262–1271,
735   https://doi.org/10.1039/d3ea00067b, 2023.

Soleimanian, E., Mousavi, A., Taghvaee, S., Sowlat, M. H., Hasheminassab, S., Polidori, A., and Sioutas, C.: Spatial trends and sources of PM2.5 organic carbon volatility fractions (OCx) across the Los Angeles Basin, Atmos. Environ., 209, 201–211, https://doi.org/10.1016/J.ATMOSENV.2019.04.027, 2019.

740   Srinivas, B. and Sarin, M. M.: Light absorbing organic aerosols (brown carbon) over the tropical Indian Ocean: Impact of biomass burning emissions, Environ. Res. Lett., 8, https://doi.org/10.1088/1748-9326/8/4/044042, 2013.

Srinivas, B. and Sarin, M. M.: Brown carbon in atmospheric outflow from the Indo-Gangetic Plain: Mass absorption efficiency and temporal variability, Atmos. Environ., 89, 835–843,
745   https://doi.org/10.1016/j.atmosenv.2014.03.030, 2014.

Sumlin, B. J., Pandey, A., Walker, M. J., Pattison, R. S., Williams, B. J., and Chakrabarty, R. K.: Atmospheric Photooxidation Diminishes Light Absorption by Primary Brown Carbon Aerosol from Biomass Burning, Environ. Sci. Technol. Lett., 4, 540–545, https://doi.org/10.1021/ACS.ESTLETT.7B00393/ASSET/IMAGES/LARGE/EZ-2017-
750   003938_0004.JPEG, 2017.

Szopa, S., Naik, V., Adhikary, B., Artaxo, P., Berntsen, T., Collins, W. D., Fuzzi, S., Gallardo, L., Kiendler Scharr, A., Klimont, Z., Liao, H., Unger, N., and Zanis, P.: Short-Lived Climate Forcers, Clim. Chang. 2021 Phys. Sci. Basis. Contrib. Work. Gr. I to Sixth Assess. Rep. Intergov. Panel Clim. Chang., 817–922,
755   https://doi.org/10.1017/9781009157896.008, 2021.

Tibrewal, K., Venkataraman, C., Phuleria, H., Joshi, V., Maithel, S., Damle, A., Gupta, A., Lokhande, P., Rabha, S., Saikia, B. K., Roy, S., Habib, G., Rathi, S., Goel, A., Ahlawat, S., Mandal, T. K., Azharuddin Hashmi, M., Qureshi, A., Dhandapani, A., Iqbal, J., Devaliya, S., Raman, R. S., Lian, Y., Pandithurai, G., Kuppili, S. K., Shiva Nagendra, M., Mukherjee, S.,
760   Chatterjee, A., Najar, T. A., Jehangir, A., Singh, J., and Sinha, B.: Reconciliation of energy use disparities in brick production in India, Nat. Sustain., 6, 1248–1257,
       https://doi.org/10.1038/s41893-023-01165-x, 2023.

Tibrewal, K., Venkataraman, C., Habib, G., Phuleria, H., Gupta, A., Gupta, G., Kumari, J., Chimurkar, N. D., Khan, S., and Singh Kapoor, T.: Country level anthropogenic emissions of
765   GHGs and air pollutants over India for 2019 from Speciated Multipollutant Generator (SMoG)-India COALESCE emissions inventory, OpenAIRE,
       https://doi.org/https://doi.org/10.5281/zenodo.10602217, 2024.

Tock, J. Y., Lai, C. L., Lee, K. T., Tan, K. T., and Bhatia, S.: Banana biomass as potential renewable energy resource: A Malaysian case study, Renew. Sustain. Energy Rev., 14, 798–
770   805, https://doi.org/10.1016/J.RSER.2009.10.010, 2010.

Tohidi, R., Altuwayjiri, A., and Sioutas, C.: Investigation of organic carbon profiles and sources of coarse PM in Los Angeles, Environ. Pollut., 314, 120264,
       https://doi.org/10.1016/J.ENVPOL.2022.120264, 2022.

Turpin, B. J., Lim, H., Turpin, B. J., and Lim, H.: Species Contributions to PM2 . 5 Mass
775   Concentrations : Revisiting Common Assumptions for Estimating Organic Mass Species Contributions to PM2 . 5 Mass Concentrations : Revisiting Common Assumptions for Estimating Organic Mass, 35(1), 602–610, https://doi.org/10.1080/02786820119445, 2001.

Venkataraman, C., Bhushan, M., Dey, S., Ganguly, D., Gupta, T., Habib, G., Kesarkar, A., Phuleria, H., and Raman, R. S.: Indian Network Project on Carbonaceous Aerosol Emissions,
780   Source Apportionment and Climate Impacts (COALESCE), Bull. Am. Meteorol. Soc., 101, E1052–E1068, https://doi.org/10.1175/BAMS-D-19-0030.1, 2020.

Vodička, P., Schwarz, J., Cusack, M., and Ždímal, V.: Detailed comparison of OC/EC aerosol at an urban and a rural Czech background site during summer and winter, Sci. Total Environ., 518–519, 424–433, https://doi.org/10.1016/J.SCITOTENV.2015.03.029, 2015.

785   Wang, Y., Hu, M., Li, X., and Xu, N.: Chemical Composition, Sources and Formation Mechanisms of Particulate Brown Carbon in the Atmosphere, Prog. Chem., 32, 627,
       https://doi.org/10.7536/PC190917, 2020.

Weyant, C., Athalye, V., Ragavan, S., Rajarathnam, U., Lalchandani, D., Maithel, S., Baum, E., and Bond, T. C.: Emissions from South Asian brick production, Environ. Sci. Technol.,
790   48, 6477–6483, https://doi.org/10.1021/ES500186G, 2014.

Yevich, R. and Logan, J. A.: An assessment of biofuel use and burning of agricultural waste in the developing world, Global Biogeochem. Cycles, 17,
       https://doi.org/10.1029/2002GB001952, 2003.

Zhang, A., Wang, Y., Zhang, Y., Weber, R. J., Song, Y., Ke, Z., and Zou, Y.: Modeling the

795   global radiative effect of brown carbon: A potentially larger heating source in the tropical
        free troposphere than black carbon, Atmos. Chem. Phys., 20, 1901–1920,
        https://doi.org/10.5194/acp-20-1901-2020, 2020.

        Zhu, Y., Wang, Q., Yang, X., Yang, N., and Wang, X.: Modeling investigation of brown
        carbon aerosol and its light absorption in China, Atmosphere (Basel)., 12, 1–12,
800   https://doi.org/10.3390/atmos12070892, 2021.